JACS Au
AN OPEN ACCESS JOURNAL OF THE AMERICAN CHEMICAL SOCIETY

pubs.acs.org/jacsau
Article

Strain-Releasing Ring-Opening Diphosphinations for the Synthesis of Diphosphine Ligands with Cyclic Backbones

Chandu G. Krishnan, Hideaki Takano, Hitomi Katsuyama, Wataru Kanna, Hiroki Hayashi, and Tsuyoshi Mita*

Cite This: JACS Au 2024, 4, 3777−3787
Read Online

ACCESS | Metrics & More | Article Recommendations | Supporting Information

ABSTRACT: Diphosphine ligands based on cyclobutane, bicyclo[3.1.1]heptane, and bicyclo[4.1.1]octane were synthesized from the corresponding highly strained, small, cyclic organic molecules, i.e., bicyclo[1.1.0]butane, [3.1.1]propellane, and [4.1.1]propellane, employing a ring-opening diphosphination. Under photocatalytic conditions, the three-component reaction of a diarylphosphine oxide, one of the aforementioned strained molecules, and a diarylchlorophosphine results in the smooth formation of the corresponding diphosphines in high yield. The obtained diphosphines can be expected to find applications in functional molecules due to their unique structural characteristics, which likely impart specific properties on their associated metal complexes and coordination polymers (e.g., a zigzag-type structure). The feasibility of the initial radical addition can be estimated using density-functional-theory calculations using the artificial force induced reaction (AFIR) method. This study focuses on the importance of integrating experimental and computational methods for the design and synthesis of new diphosphination reactions that involve strained, small, cyclic organic molecules.

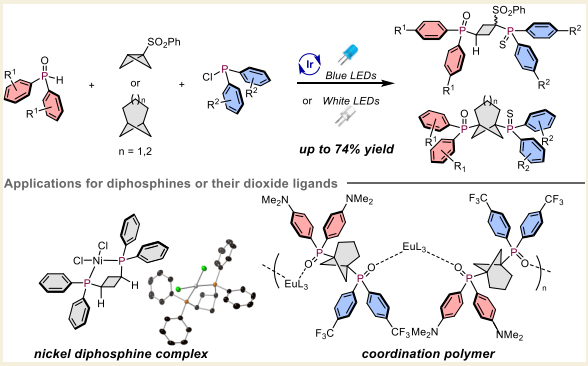

KEYWORDS: *radical, diphosphine ligands, blue LED, strained molecules, propellane*

INTRODUCTION

Significant advancements in the development of novel functionalized materials, such as phosphine ligands, have recently been reported.[1,2] At present, one fascinating avenue of exploration in this area is the synthesis of diphosphine ligands that coordinate to metal centers in either a bidentate or monodentate fashion. Diphosphine ligands with a bidentate coordination mode allow the formation of metallacycles, which are stabilized by chelation effects,[3,4] while those with a monodentate mode serve as molecular linkers, resulting in the formation of supramolecular assemblies.[5−12] The reactivity of diphosphine ligands is primarily contingent upon two crucial parameters: the cone angle[13−15] and the bite angle.[3,4] These angles can be precisely tailored by leveraging the steric effects stemming from the substituents on the phosphorus atoms and the backbone linkers that connect the two phosphorus atoms (Scheme 1a). In the case of the substituents on the phosphorus atoms, electronic effects are also pivotal in orchestrating the reactivity of the metal complex. Unsymmetric diphosphine ligands that carry different substituents on each phosphorus atom, may have, through a judicious selection of substituents, potentially exceptional reactivity profiles. Consider, for instance, a diphosphine ligand where one phosphorus atom bears electron-donating groups, while its counterpart bears electron-withdrawing moieties.

This configuration can be expected to endow the ligand with distinctive reactivity and properties compared to its symmetric counterparts. Such modified reactivity and properties arise from the push−pull effect, which contributes to the precise modulation of electron density on the central metal atom. Indeed, unsymmetric diphosphine ligands have, on occasion, demonstrated an enhanced capacity to augment the reactivity, regioselectivity, and enantioselectivity of transition-metal-catalyzed reactions when compared to their symmetrical counterparts.[16−21] Consequently, both the architecture of the backbone linkers and the nature of the substituents attached to the phosphorus atoms wield substantial influence over the reactivity of diphosphine metal complexes. This underscores the pressing need for facile and universally applicable methods for the synthesis of both symmetric and unsymmetric diphosphine ligands with a diverse array of carbon frameworks.

Small cyclic hydrocarbons can exhibit substantial ring strain, that primarily stems from the unconventional bond angles

Received: April 18, 2024
Revised: July 16, 2024
Accepted: July 17, 2024
Published: July 29, 2024

Scheme 1. Importance of Bidentate Phosphine Ligands

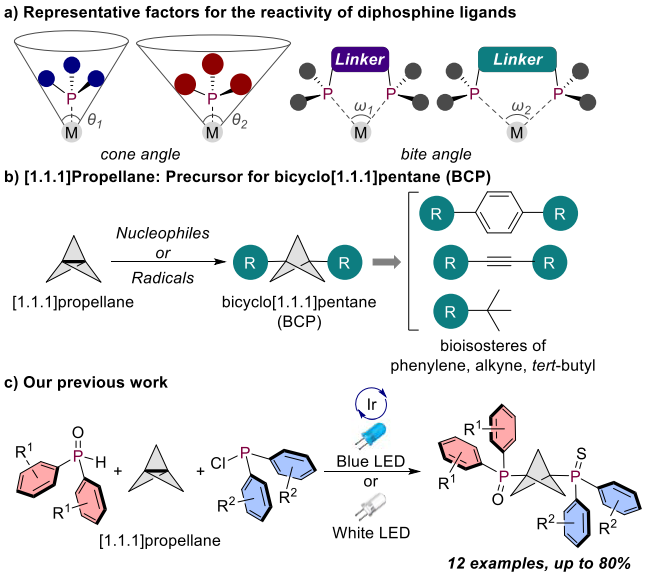

adopted by the sp^3-hybridized carbon atoms.[22−24] In recent years, considerable research attention has been devoted to polycyclic hydrocarbons, bicyclo[1.1.0]butane,[25−32] and propellanes.[33−49] These intriguing compounds are characterized by two or three interconnected rings, each sharing a common C−C bond. [1.1.1]Propellane[32−44] has garnered significant interest due to its high reactivity with cations, anions, and radicals. This heightened reactivity can be attributed to the exceptionally strained C−C bonds between the bridgehead carbons (charge-shift bonds). The reaction of [1.1.1]-propellane with an anion or a radical leads to a bicyclo[1.1.1]-pentane (BCP) skeleton, which represents a biological isostere of benzene rings, alkynes, or *tert*-butyl groups (Scheme 1b).[50−54] Notably, our research group has previously reported a three-component reaction (3CR) for the synthesis of symmetric/unsymmetric diphosphine ligands,[55,56] and one of these ligands is a straight-shaped diphosphine derived from [1.1.1]propellane (Scheme 1c).[56] The key to this significant synthetic advancement lies in the 3CR strategy, where a diarylphosphine oxide, a highly strained hydrocarbon scaffold, and a diarylchlorophosphine can be assembled under photocatalytic conditions.

Taking into consideration the reactivity of highly strained small-ring compounds and the utility of the three-dimensional hydrocarbon structures generated from their reactions, the development of a 3CR involving small-ring compounds would facilitate the creation of novel functional diphosphine ligands. In the present study, we have determined the activation barriers for the addition of electron-withdrawing phosphoryl radicals ($Ph_2P(=O)\cdot$) to seven strained hydrocarbon molecules based on cyclopropane, bicyclo[1.1.0]butane, [n.1.1]-propellane, and [n.n.n]propellane scaffolds (Scheme 2). Based on these calculated results, we successfully synthesized several diphosphine ligands via a 3CR using the strained hydrocarbons bicyclo[1.1.0]butane,[25−32] [3.1.1]propellane,[43,45,46] and [4.1.1]propellane.[47−49]

RESULTS AND DISCUSSION

Prior to conducting experimental trials of the diphosphination procedures, our investigation commenced with density-functional-theory (DFT) calculations using the artificial force

Scheme 2. 3CR for the Synthesis of Diphosphine Ligands

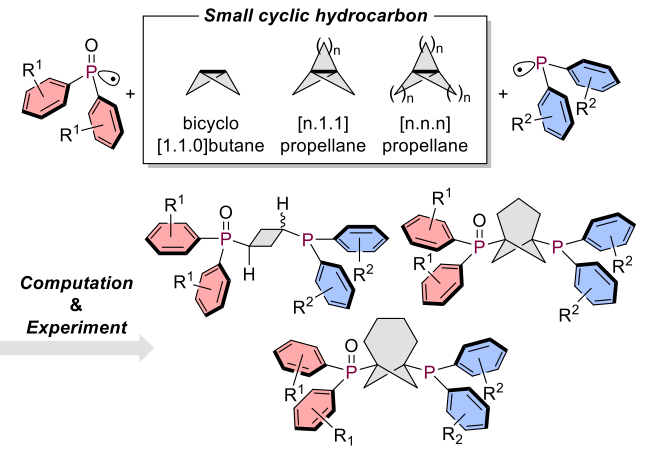

induced reaction (AFIR) method[57−60] at the UωB97X-D/Def2-SVP level in dichloromethane (SMD model). Subsequently, we directed our attention to simulating the addition of the phosphoryl radical ($Ph_2P(=O)\cdot$, **1′**) to different highly strained molecules (Table 1). We calculated the energies of the two species independently, assuming that the phosphoryl radical and the substrate are infinitely far apart. We then combined these energies, which serves as the reference for

Table 1. DFT-Calculated Activation Barriers for the Addition of a Phosphoryl Radical to Strained Molecules

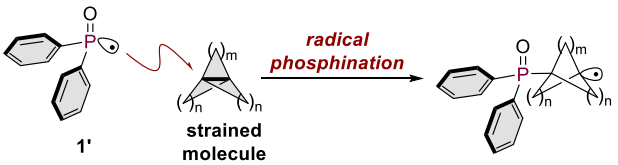

entry	substrate	ΔG‡	ΔG	entry	substrate	ΔG‡	ΔG
1		30.3	−8.9	6		**8.1**	−19.6
2		**14.0**	−21.3	7		12.0	−18.5
3	 previous work	8.5	−11.0	8		**9.2**	−16.8
4		**5.7**	−34.2	9		**12.2**	−54.1
5		13.4	−20.3	10		54.9	23.0

potentially reactive substrates


bicyclo[1.1.0]butane


[2.1.1]propellane
not stable to isolate


[3.1.1]propellane


[4.1.1]propellane


[2.2.2]propellane
not stable to isolate

https://doi.org/10.1021/jacsau.4c00347
JACS Au 2024, 4, 3777−3787

drawing an energy diagram. The phosphoryl radical exhibits greater reactivity toward hydrocarbons than the phosphinyl radical ($Ph_2P\cdot$) because the electron-withdrawing radical prefers to react with electron-rich hydrocarbon substrates (for details, see the Supporting Information (S37)). The phosphoryl radical can be readily generated via photoirradiation from the *in situ*-formed diphosphine oxide ($Ph_2P(=O)-PPh_2$) derived from the phosphine oxide ($Ph_2P(=O)H$) and the chlorophosphine (Ph_2PCl).[55,56]

We first performed calculations for the addition of a phosphoryl radical to the simple ring-strained molecule cyclopropane, which was found to have an extremely high activation barrier ($\Delta G^{\ddagger}$ = 30.3 kcal/mol; entry 1). In contrast, bicyclo[1.1.0]butane[25−32] has a much lower activation barrier ($\Delta G^{\ddagger}$ = 14.0 kcal/mol; entry 2). As calculated in our previous study, [1.1.1]propellane[33−44] has a reasonably low activation barrier ($\Delta G^{\ddagger}$ = 8.5 kcal/mol; entry 3). The calculations performed for the reaction with [2.1.1]propellane[61] revealed the lowest activation barrier ($\Delta G^{\ddagger}$ = 5.7 kcal/mol) of the compounds shown in Table 1 (entry 4). Unsymmetric propellanes, such as [3.1.1]propellane[43,45,46] and [4.1.1]propellane,[47−49] have two geometries that the phosphoryl radical can access, with a large difference in activation barriers between the two paths. One geometry has a low barrier while the other has a high barrier (entries 5−8). The geometries where the bulky cyclopentane or cyclohexane faces the same direction as the oxygen atom of the phosphoryl radical have higher activation barriers ($\Delta G^{\ddagger}$ = 13.4 and 12.0 kcal/mol; entries 5 and 7). Conversely, when the cyclic hydrocarbon is orientated in the opposite direction to the oxygen atom of the phosphoryl radical, a much lower activation barrier is observed ($\Delta G^{\ddagger}$ = 8.1 and 9.2 kcal/mol; entries 6 and 8). We also performed calculations for the reactions of [2.2.2]propellane[62,63] and [3.3.3]propellane,[64,65] which revealed that the former exhibits a reasonable activation barrier ($\Delta G^{\ddagger}$ = 12.2 kcal/mol), while the latter has a very high activation barrier ($\Delta G^{\ddagger}$ = 54.9 kcal/mol) with an endergonic reaction profile (entries 9 and 10). Based on these calculations, all listed strained compounds, except cyclopropane and [3.3.3]propellane, exhibit reasonable activation barriers. However, [2.1.1]propellane[61] and [2.2.2]propellane[62,63] have been reported to be insufficiently stable toward isolation (*vide infra*), and the diphosphination of [1.1.1]propellane has been already reported by our research group.[56] Therefore, we focused on experimentally verifying the diphosphination of bicyclo[1.1.0]butane,[25−32] [3.1.1]propellane,[43,45,46] and [4.1.1]propellane,[47−49] in addition to the confirmation of the nonreactivity of cyclopropane.

Cyclopropane

As expected, given the formidable activation barrier ($\Delta G^{\ddagger}$ = 30.3 kcal/mol) estimated by DFT calculations (vide supra), several attempts at the 3CR involving the opening of cyclopropane (10% in N_2 gas under 10 atm pressure) using phosphine oxide **1** and chlorophosphine **2** were unsuccessful (Figure 1). Instead of the targeted 1,2-bis(diarylphosphino)-propane derivatives, unsymmetric and symmetric diphosphines **3aa** and **3bb** were obtained in a ca. 20% yield.

Bicyclo[1.1.0]butane

Next, we examined the 3CR involving bicyclo[1.1.0]butane because its calculated activation barrier is reasonably low ($\Delta G^{\ddagger}$ = 14.0 kcal/mol). Bicyclo[1.1.0]butane was prepared as a Et_2O solution according to a slightly modified literature procedure[28]

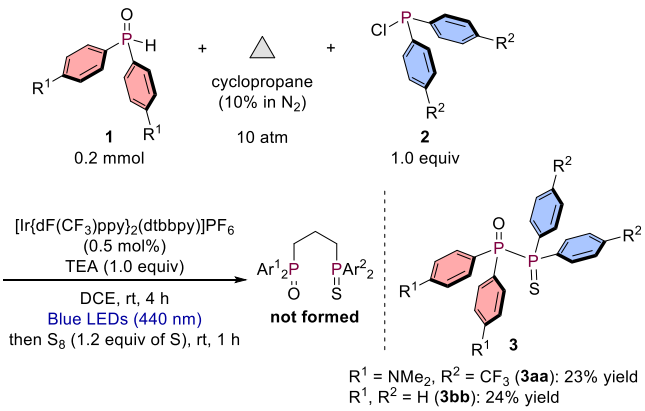

Figure 1. 3CR of cyclopropane with **1** and **2**.

(for details, see the Supporting Information (S3)). Unfortunately, when using (p-NMe_2-C_6H_4)$_2$P(=O)H (**1a**) and (p-CF_3−C_6H_4)$_2$PCl (**2a**) as substrates for the 3CR with bicyclo[1.1.0]butane, several unidentified compounds were formed, while the formation of the targeted unsymmetric **4aa** was not observed. Instead of the generation of **4aa**, diphosphine **3aa** was obtained in 37% yield (Figure 2).

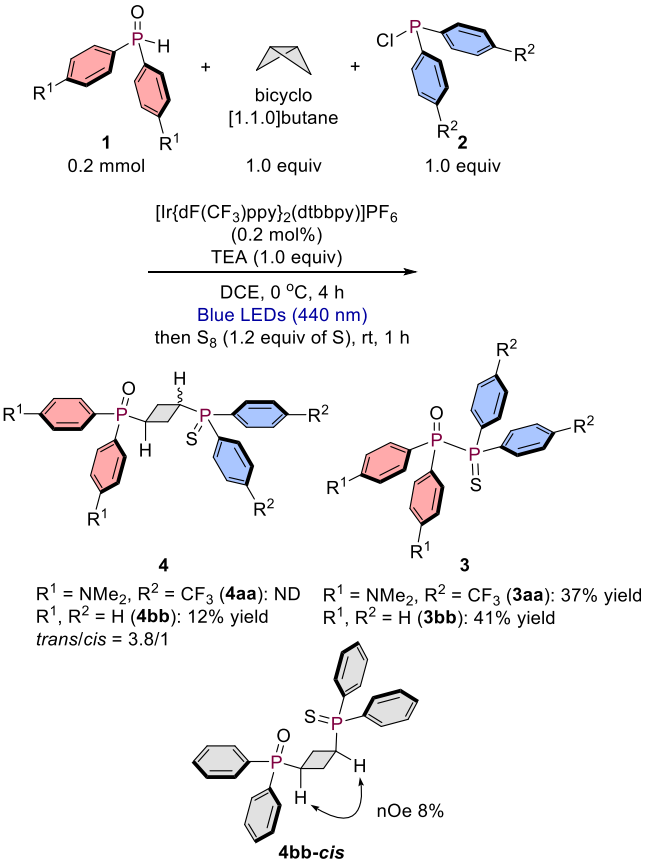

Figure 2. 3CR of bicyclo[1.1.0]butane.

However, when $Ph_2P(=O)H$ (**1b**) and Ph_2PCl (**2b**) were used as substrates, symmetric derivative **4bb** was obtained in 12% yield with a *trans*/*cis* ratio of 3.8/1 together with diphosphine **3bb** in 41% yield. The structure of the minor **4bb-*cis*** isomer was determined by an nOe experiment with an 8% correlation (for details, see the Supporting Information (S17)).

https://doi.org/10.1021/jacsau.4c00347
JACS Au 2024, 4, 3777−3787

Despite obtaining a small amount of **4bb**, a substantial quantity of unidentified byproducts were formed, probably due to the generation of rather reactive secondary radicals after the addition of the phosphoryl radical. Moreover, as bicyclo[1.1.0]butane is a gaseous substance that could potentially evaporate during light irradiation (the reported bp is 8 °C[27]), it was decided to use a solid bicyclobutane, which does not evaporate and is easier to handle. Benzensulfonyl-substituted bicyclo[1.1.0]butane (**5**), which is readily prepared from inexpensive benzenesulfinic acid sodium salt and 4-bromobut-1-ene,[34] was subsequently employed for the 3CR. The sulfonyl group can be readily removed under reductive conditions. The activation barrier of the addition of phosphoryl radical **1′** to **5** ($\Delta G^{\ddagger}$ = 15.2 kcal/mol) is sufficient to allow experiments to be conducted. As a result, the product yields increased compared to when bicyclo[1.1.0]butane was used, and unsymmetric **6aa** was obtained in 23% yield (*cis*/*trans* = 1.6/1) and symmetric derivative **6bb** in 53% yield (*cis*/*trans* = 4/1) (Figure 3). A 0.7 mmol-scale reaction also worked

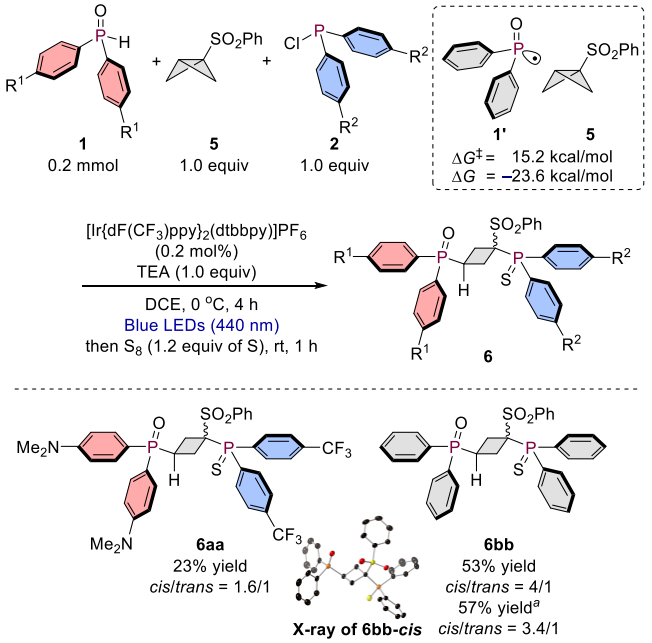

Figure 3. 3CR of sulfonylated bicyclo[1.1.0]butane. [a]0.7 mmol-scale synthesis.

well, resulting in the formation of **6bb** in 57% yield with a *cis*/*trans* ratio of 3.4/1. The major diastereomer of **6bb** was unambiguously determined to have a *cis* configuration via X-ray diffraction (XRD) analysis of a suitable single crystal.[66]

The sulfonylated compound **6bb** (*cis*/*trans* mixture) was smoothly desulfonylated using Mg powder in the presence of $NiBr_2$ (20 mol %) to afford the target molecule **4bb** in good yield (Figure 4). In this process, the stereochemistry of **6bb** was not maintained, affording **4bb** with a *trans*/*cis* ratio that was different to the original ratio of **6bb**. As the desired Mg-mediated process involves a radical process, the resulting secondary radial formed after the desulfonylation undergoes epimerization to give **4bb** in an almost 1:1 *trans*/*cis* ratio. In the case of unsymmetric **6aa**, a significantly simultaneous defluorination of the CF_3 group occurred during the desulfonylation, and the reductive desulfonylation with Mg

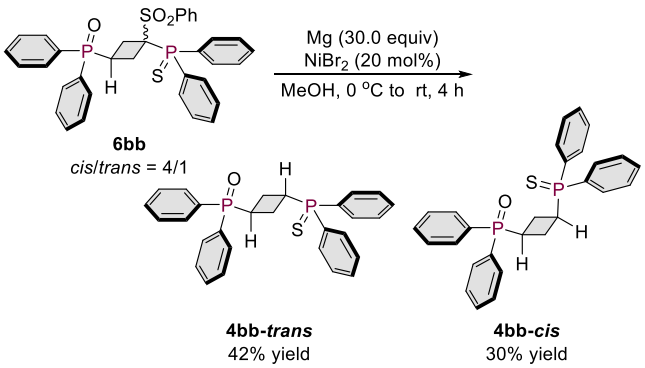

Figure 4. Removal of the sulfonyl group under Mg-mediated conditions.

was therefore deemed to be unsuitable for CF_3-containing compounds.

We then investigated the use of **4bb-*cis*** in the synthesis of a *cis*-coordinate bidentate ligand (Figure 5). After oxidative

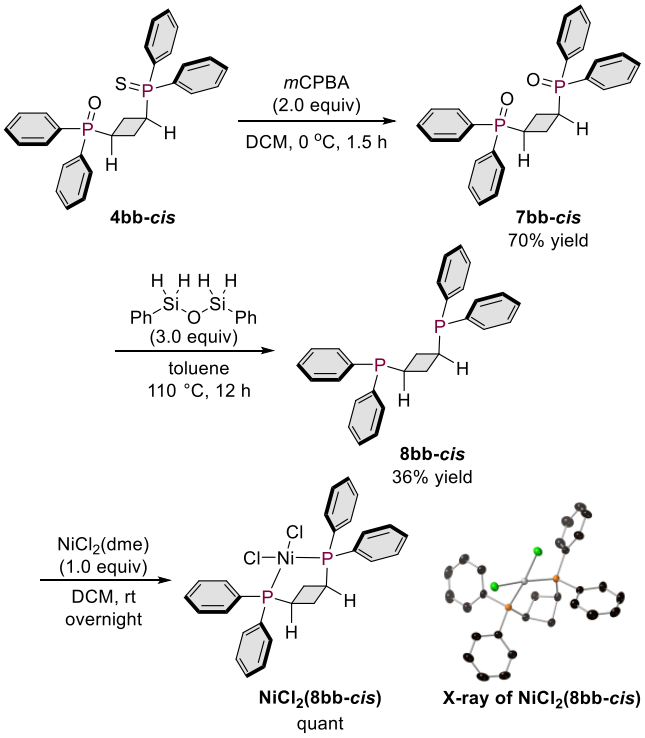

Figure 5. Conversion of **4bb-*cis*** to *cis*-coordinate Ni-complex **$NiCl_2$(8bb-*cis*)**. Bottom right: crystal structure of **$NiCl_2$(8bb-*cis*)** with thermal ellipsoids at 50% probability; all hydrogen atoms as well as one molecule of CH_2Cl_2 have been omitted for clarity.

exchange of the S atom on the phosphine sulfide moiety of **4bb-*cis*** with an O atom via treatment with *m*CPBA, the corresponding dioxide **7bb-*cis*** was obtained in 70% yield. **7bb-*cis*** was readily reduced using air-stable 1,3-diphenyl-disiloxane ($PhH_2Si-O-SiH_2Ph$; DPDS)[67,68] in toluene under reflux conditions without the need for a glovebox to afford **8bb-*cis*** in 36% yield. The obtained **8bb-*cis*** reacts with $NiCl_2$(dme) to form a red powder of **$NiCl_2$(8bb-*cis*)**. Recrystallization from CH_2Cl_2/hexane yielded red/orange single crystals that contain one molecule of CH_2Cl_2 per unit cell. A single-crystal X-ray diffraction analysis revealed a bidentate chelating coordination

https://doi.org/10.1021/jacsau.4c00347
JACS Au 2024, 4, 3777−3787

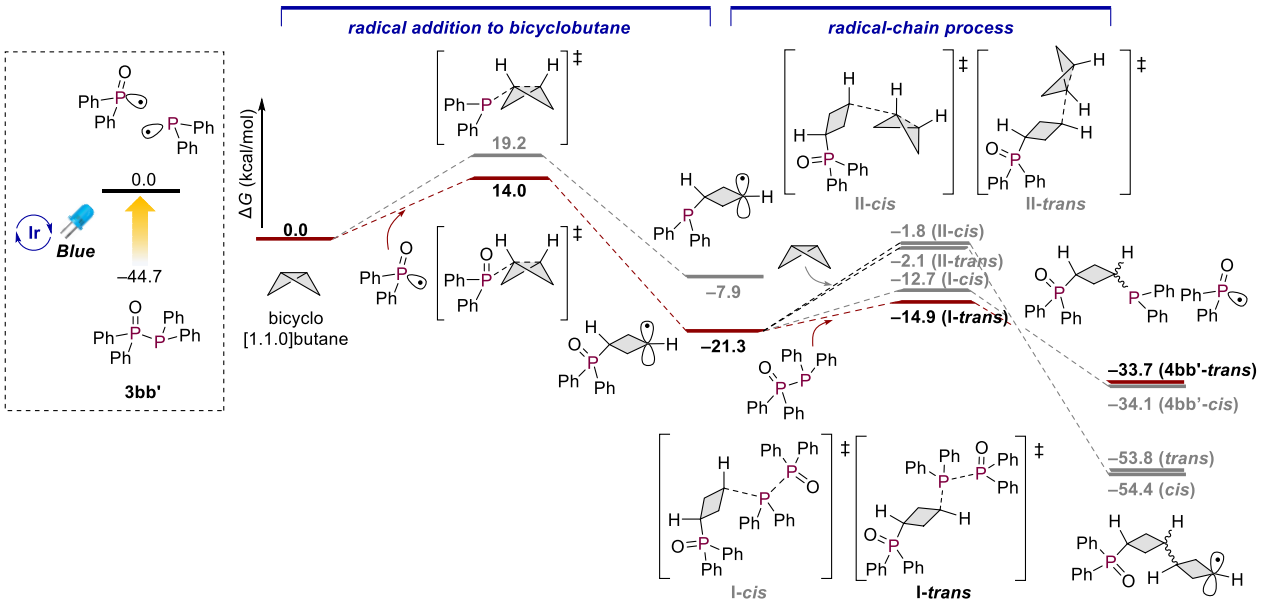

Figure 6. Plausible reaction mechanism based on DFT calculations for the 3CR with bicyclo[1.1.0]butane. The reaction diagrams were calculated at the UωB97X-D/Def2-SVP/SMD(DCM) level.

of the diphosphine to Ni with a cyclobutane backbone.[66] It should be noted here that the cyclobutane ring is slightly distorted, most likely as a result of the propensity of the ligand to form a chelate. This type of chelating diphosphine-metal complex has not been reported so far; interestingly, while the number of bridging carbon atoms is the same as in dppp (three carbons), the bite angle is larger. Specifically, the X-ray structure reveals that its bite angle is 94.95 °, thus exceeding the reported value for dppp in $NiCl_2$(dppp) (91.77 °).[69] This difference should most likely be attributed to the reduced flexibility of the carbon chain caused by the constrained cyclobutane ring, suggesting potential for future applications in catalysis.[1−4]

Subsequently, we conducted a theoretical examination of the mechanism of the light-promoted radical reaction in order to investigate the *trans*-selectivity. For that purpose, we carried out DFT calculations using $Ph_2P(=O)-PPh_2$ (**3bb′**), which should be initially generated from **1b** and **2b** in the presence of a base (Figure 6). When using **3bb′** for the reaction with **5**, **6bb** was obtained in similar yield (48% yield), which indicates **3bb′** is an intermediate of this radical reaction. The calculations were again conducted using the AFIR method[57−60] at the UωB97X-D/Def2-SVP level in dichloromethane (SMD model) (for details, see the Supporting Information (S36)). Under blue LED irradiation, [Ir{dF(CF_3)ppy}$_2$(dtbbpy)]PF_6 absorbs light at 440 nm and is excited to its triplet state (ΔE^T = 61.8 kcal/mol),[70] which then transfers energy to **3bb′**, which in turn is excited to the triplet state (ΔG = 44.7 kcal/mol).[56] Simultaneous dissociation of the P(=O)−P single bond occurs from the triplet state of **3bb′**, and the resulting phosphoryl radical ($Ph_2P(=O)\cdot$) reacts with bicyclo[1.1.0]butane to generate a secondary-alkyl radical ($\Delta G^{‡}$ = 14.0 kcal/mol). When radical addition occurs with the phosphinyl radical ($Ph_2P\cdot$) instead of with the phosphoryl radical, the resulting activation barrier is higher ($\Delta G^{‡}$ = 19.2 kcal/mol vs 14.0 kcal/mol). The thus obtained secondary-alkyl radical may react associatively with the remaining phosphinyl radical (radical−radical coupling) to afford the target molecule **4bb′**.

However, both the secondary-alkyl radical and the phosphinyl radical exhibit transient character,[71] and they seem to be present at low concentrations. Therefore, we calculated another possibility involving a radical-chain mechanism, which revealed an activation barrier of 6.4 kcal/mol for the radical addition of the secondary-alkyl radical to another molecule of diphosphine **3bb′** in a *trans*-selective fashion through **I-*trans***. However, the *cis*-selective phosphination via **I-*cis*** proceeds with a bit higher activation energy (8.6 kcal/mol). Accordingly, both paths could give the products with an exergonic energy profile. Based on the activation barrier for the radical-chain addition, which can be reasonably overcome at room temperature, we currently consider that the radical-chain process may be operative, even though the termination process with radical−radical coupling can also be expected to be operative in the system, similar to the case of [1.1.1]propellane.[56] We also conducted calculations for the reaction of the secondary-alkyl radical with another molecule of bicyclo[1.1.0]butane. Our calculations indicate that the activation barriers for the radical dimerization of bicyclo[1.1.0]butane via **II-*trans*** and **II-*cis*** are higher than that of the anticipated radical-chain pathway ($\Delta G^{‡}$ = 19.2/19.5 kcal/mol (*trans*/*cis* for dimerization) vs 6.4/8.6 kcal/mol (*trans*/*cis* for product formation)), effectively ruling out the possibility of product polymerization.

[1.1.1]Propellane and [2.1.1]Propellane

Our research group has previously reported the diphosphination of [1.1.1]propellane.[56] In contrast, [2.1.1]propellane, distinguished by a central carbon atom bonded to one cyclobutane ring and two cyclopropane rings, is known to be unstable and difficult to isolate, rendering its synthesis exceedingly difficult.[48,61]

[3.1.1]Propellane

Subsequently, our investigation shifted toward [3.1.1]propellane as a substrate for the 3CR given its suitably low activation barrier ($\Delta G^{‡}$ = 8.1 kcal/mol). We investigated the reaction of **1** with [3.1.1]propellane and **2** and were able to successfully synthesize several diphosphines (Figure 7). This

https://doi.org/10.1021/jacsau.4c00347
JACS Au 2024, 4, 3777−3787

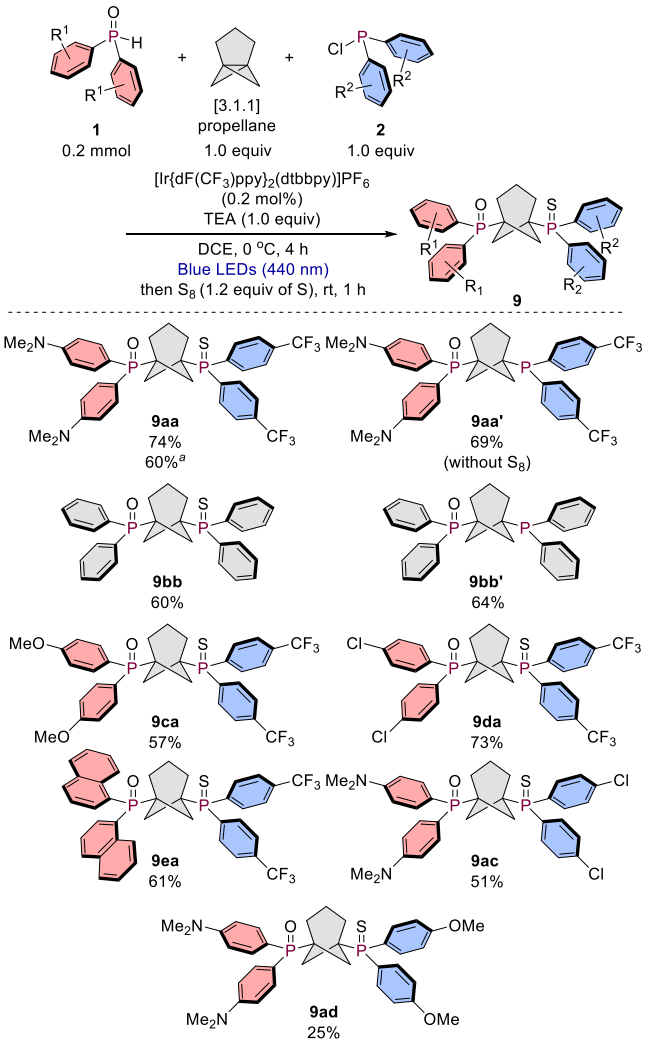

Figure 7. 3CR of [3.1.1]propellane. [a]White LED irradiation for 24 h without a photocatalyst.

synthetic process yielded both unsymmetric and symmetric diphosphine derivatives **9** in yields of up to 74%. A variety of electron-donating phosphine oxides and electron-withdrawing chlorophosphines can be used in this 3CR. We first examined the electron-donating phosphine oxide (p-NMe_2-C_6H_4)$_2$P(=O)H (**1a**) and electron-deficient chlorophosphine (p-CF_3–C_6H_4)$_2$PCl (**2a**) under photochemical reaction conditions. Under photocatalytic conditions using blue LED irradiation, the unsymmetric diphosphine derivative **9aa** was obtained in 74% yield. The 3CR also proceeded without the need for a photocatalyst under white LED irradiation for 24 h, which is similar to reaction conditions that we have developed previously.[55,56] Without protection using S_8, **9aa′** was obtained in a similar yield (69%). Symmetric derivative **9bb** was prepared from **1b** and **2b** in 60% yield. Without sulfur protection, **9bb′** was obtained in 64% yield. We then continued to extend the substrate scope. For that purpose, we screened various electron-donating phosphine oxides in the reaction with the electron-withdrawing chlorophosphine **2a**. The 3CR between electron-donating (p-OMe-C_6H_4)$_2$P(=O)H (**1c**) and **2a** proceeded well under otherwise identical conditions. Furthermore, the 3CR with electron-withdrawing (p–Cl-C_6H_4)$_2$P(=O)H (**1d**) and bulky (1-naphthyl)$_2$P(=O)H (**1e**) proceeded smoothly. Next, electron-donating **1a** was used as the phosphine oxide and several chlorophosphines were screened. Electron-withdrawing (p–Cl-C_6H_4)$_2$PCl (**2c**) afforded the desired product **9ac** in moderate yield. Furthermore, the use of electron-donating (p-OMe-C_6H_4)$_2$PCl (**2d**) provided **9ad**, albeit that the yield was somewhat low (25%).

Next, we embarked on an in-depth exploration of the transformation of both **9aa** and **9bb** into their corresponding diphosphine dioxide derivatives, i.e., **10aa** and **10bb**. We also examined the subsequent production of diphosphine ligands **11aa** and **11bb** from **10aa** and **10bb** (Figure 8). The reaction process began with the oxidative substitution of the sulfur atoms on the phosphine sulfide moiety with oxygen atoms, achieved via treatment with mCPBA, which led to the synthesis of the targeted diphosphine dioxide compounds **10** in reasonable yield. Subsequently, the thus obtained diphosphine dioxides **10** underwent reduction by air-stable DPDS[67,68] in toluene under reflux conditions. This reduction proved efficient, yielding unsymmetric and symmetric diphosphine ligands **11** in good yield, thus underscoring the robustness and versatility of the synthetic methodology employed.

Another notable result is the possibility to subsequently using the unsymmetric dioxide **10aa** in the synthesis of a novel Eu-based coordination polymer **12** via the reaction with $Eu(hfa)_3(H_2O)_2$ (hfa = hexafluoroacetylacetonate). The resulting coordination polymer **12** was obtained in 39% yield after crystallization. A detailed single-crystal X-ray diffraction (XRD) analysis unambiguously confirmed the coordination mode of the europium ions within polymer **12**.[66] In **12**, each europium ion is intricately coordinated by three hfa ligands and two phosphine-oxide ligands. Notably, each phosphine-oxide moiety in the ligand exhibits different electronic characteristics, i.e., one is electron-donating and the other electron-withdrawing. An octacoordinated metal center, which is similar to the coordination polymer **12′** derived from [1.1.1]propellane,[56] is formed. However, the packing structure of polymer **12** differs significantly from that of the polymer **12′**. While **12′** forms an approximately straight-shaped wire, **12** exhibits a wire-shaped structure with zigzag bends on the same plane (Figure 8), wherein the bends to ∼98° occur every three Eu centers.

This structural difference arises from variances in the linker structures. Two C–P bonds are positioned in nearly the same straight line (174°) due to the linkage of the BCP skeleton. Conversely, the [3.1.1]bicycloheptane skeleton introduces two C–P bonds at a specific angle (117°), which most likely influences the zigzag structure in the crystal packing. However, the intrinsic origin of the bent structure for every three Eu units remains unexplained at present. The resulting polymeric architecture, dictated by this unique coordination pattern and the packing structure, showcases exceptional alignment, thereby establishing a promising framework with potential applications in the realm of luminescent photonic materials. Our ongoing research in this area is focused on exploring the optical properties of this intriguing polymeric complex.

We subsequently conducted a theoretical examination of the mechanism of the light-promoted radical reaction of [3.1.1]-propellane, supported by DFT calculations (Figure 9). In this substrate, not only blue LED light but also white LED light without any photocatalyst proves suitable for promoting the reaction (cf. **9aa** in Figure 7).[55,56] Under white LED irradiation, **3bb′** directly absorbs light to facilitate its radical-dissociation reaction. After the homolytic cleavage of the P(=

https://doi.org/10.1021/jacsau.4c00347
JACS Au 2024, 4, 3777–3787

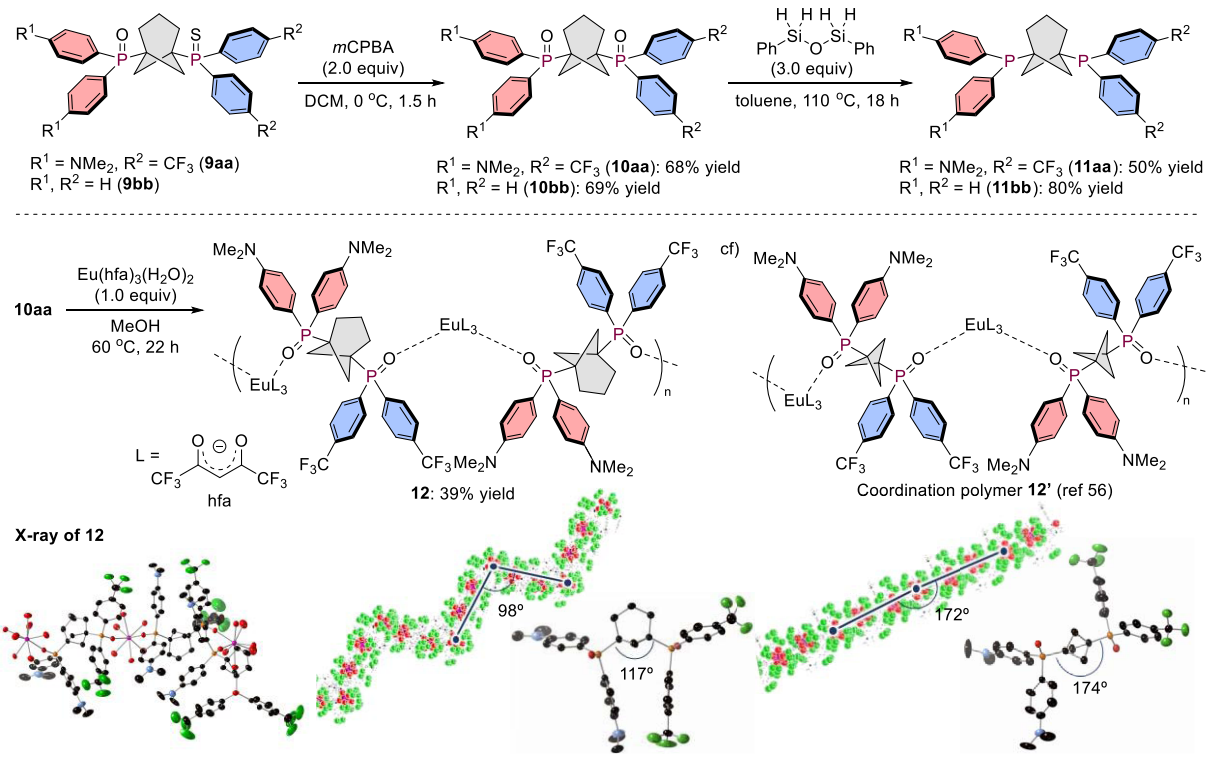

Figure 8. Synthesis of diphosphine ligands and metal complexes. Bottom right: crystal structures of **12** and **12′** with thermal ellipsoids at 30% probability; fluorine atoms on the hfa ligands and all hydrogen atoms are omitted for clarity.

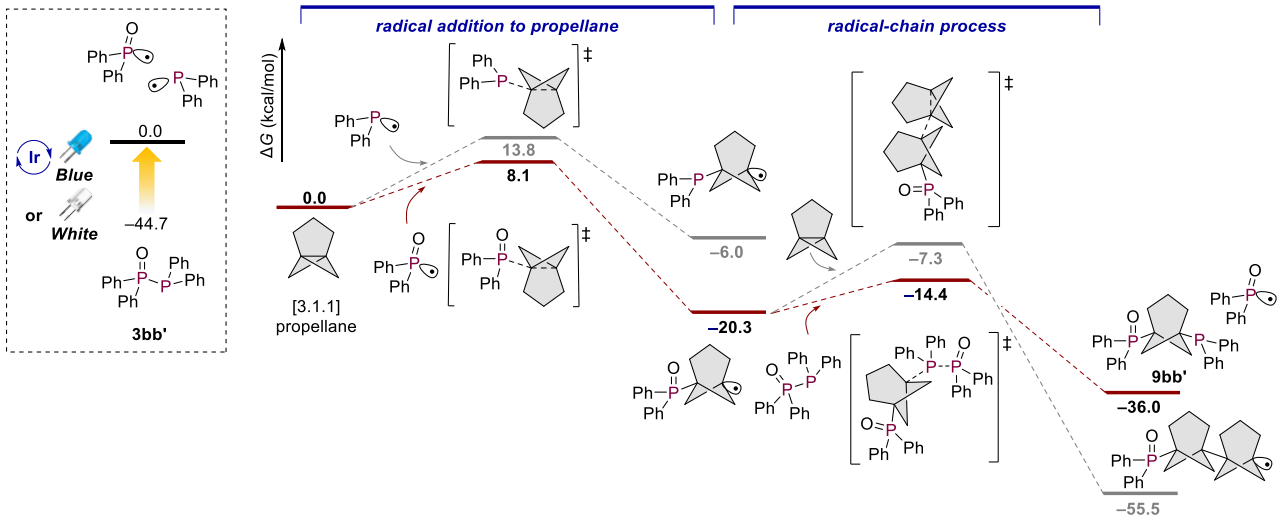

Figure 9. Plausible reaction mechanism based on DFT calculations for the 3CR with [3.1.1]propellane. The reaction diagrams were calculated at the UωB97X-D/Def2-SVP/SMD(DCM) level.

O)−P single bond, phosphoryl radical ($Ph_2P(=O)\cdot$) reacts with [3.1.1]propellane to generate a tertiary-alkyl radical ($\Delta G^{\ddagger}$ = 8.1 kcal/mol). When radical addition occurs with the phosphinyl radical ($Ph_2P\cdot$) instead of the phosphoryl radical, the resulting activation barrier is higher ($\Delta G^{\ddagger}$ = 13.8 kcal/mol vs 8.1 kcal/mol). The tertiary-alkyl radical thus obtained may undergo an associative reaction with the remaining phosphinyl radical (radical−radical coupling) to yield the target molecule **9bb′**. We also explored another possibility involving a radical-chain mechanism, which revealed an activation barrier of 5.9 kcal/mol for the radical addition of the tertiary-alkyl radical to another molecule of diphosphine **3bb′**. Considering the low likelihood of an encounter between the two radical species discussed above, in this case we also believe that the radical-chain process may be operative together with radical−radical coupling during the termination process.[56] We also conducted calculations for the reaction of the tertiary-alkyl radical with another molecule of [3.1.1]propellane, indicating that the activation barrier for the radical dimerization of [3.1.1]-propellane is higher than that of the anticipated radical-chain pathway ($\Delta G^{\ddagger}$ = 13.0 kcal/mol vs 5.9 kcal/mol), which prevents the dimerization with another [3.1.1]propellane.

https://doi.org/10.1021/jacsau.4c00347
JACS Au 2024, 4, 3777−3787

[4.1.1]Propellane

[4.1.1]Propellane is a fused compound that has already been synthesized.[47−49] However, our slightly modified method using PhLi-mediated cyclization leads to a robust and reproducible synthetic procedure for the synthesis of [4.1.1]propellane (for details, see the Supporting Information (S10)). Due to the reasonably favorable activation barrier for the process ($\Delta G^{\ddagger}$ = 9.2 kcal/mol), we mixed phosphine oxide **1** with [4.1.1]-propellane and chlorophosphine **2**, which resulted in the formation of diphosphines **13aa** and **13bb** in good yield (Figure 10). Furthermore, similar to the [3.1.1]propellane

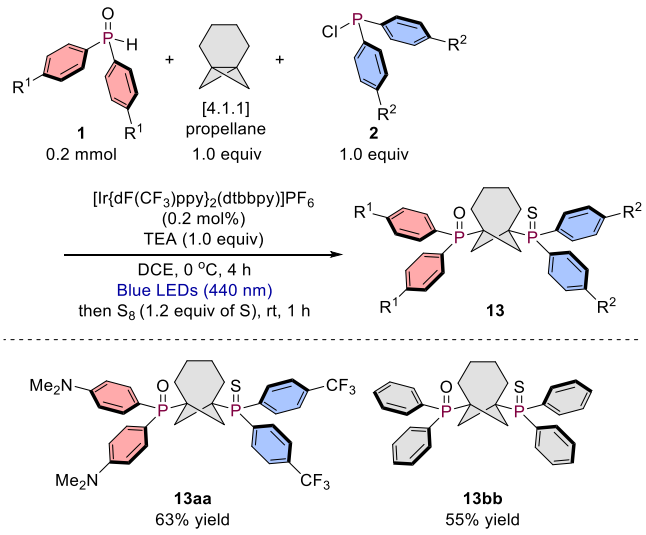

Figure 10. 3CR of [4.1.1]propellane.

synthesis, S to O exchange by *m*CPBA followed by reduction using air-stable DPDS[67,68] afforded unsymmetric and symmetric free diphosphine ligands **15aa** and **15bb** in good yields (Figure 11).

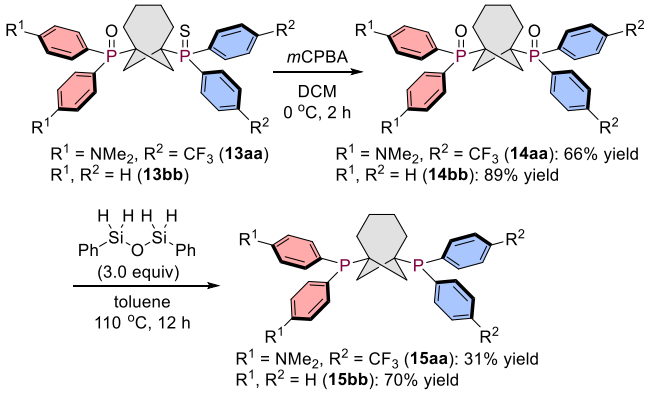

Figure 11. Conversion to free diphosphine ligands.

We further calculated the pathway of the reaction of **3bb′** with [4.1.1]propellane (Figure 12). The generated phosphoryl radical ($Ph_2P(=O)\cdot$) reacts with [4.1.1]propellane to generate the tertiary-alkyl radical ($\Delta G^{\ddagger}$ = 9.2 kcal/mol). The activation energy for the reaction with the phosphinyl radical ($Ph_2P\cdot$) is higher than that for the reaction with the phosphoryl radical ($\Delta G^{\ddagger}$ = 17.2 kcal/mol). Compared to the radical addition to [3.1.1]propellane, the activation barriers for the reaction with [4.1.1]propellane are slightly higher. The radical-chain mechanism, whereby an additional molecule of **3bb′** reacts with the tertiary-alkyl radical, which leads to the formation of **13bb′**, has a reasonable activation barrier of 8.4 kcal/mol. However, the activation barrier for the pathway where the tertiary-alkyl radical reacts with another molecule of [4.1.1]-propellane is higher than that for the generation of **13bb′** ($\Delta G^{\ddagger}$ = 16.8 kcal/mol vs 8.4 kcal/mol), which is similar to the case of [3.1.1]propellane. This result indicates that selective product formation occurs along the possible reaction pathways examined here.

[2.2.2]Propellane and [3.3.3]Propellane

[2.2.2]Propellane, characterized by a central carbon atom bonded to three cyclobutane rings, is notoriously unstable, making its synthesis formidably challenging. Numerous attempts to synthesize [2.2.2]propellane have been made to date, but regrettably, all of these endeavors have met with failure due to the thermal instability of [2.2.2]propellane.[62,63] On the other hand, the synthesis of [3.3.3]propellane, which features a central carbon atom connected to three cyclopentane rings in a slightly different arrangement, has been shown to be possible,[64,65] and the existing literature provides a viable synthetic route to [3.3.3]propellane.[64,65] However, the calculated activation barriers shown in Table 1 revealed that achieving diphosphination for this molecule would be highly unlikely due to a high activation barrier and an endergonic reaction pathway. Consequently, we have decided to forego the synthesis of [3.3.3]propellane due to the unfavorable energy profile.

CONCLUSIONS

In conclusion, this research represents a remarkable achievement in the synthesis of strained hydrocarbon-based diphosphine ligands, including diphosphinated cyclobutane, bicyclo[3.1.1]heptane, and bicyclo[4.1.1]octane, as evident by our rigorous DFT calculations. Furthermore, the results presented here hold immense promise for various potential applications in functional molecules. For example, a bicyclo[1.1.0]butane-derived *cis*-coordinated diphosphine was transformed into the corresponding Ni-complex, wherein the bite angle is wider than that in the structurally closely related complex $NiCl_2$(dppp). Moreover, a [3.1.1]propellane-derived diphosphine dioxide was transformed into a unique Eu-based coordination polymer that exhibits a zigzag-type polymeric structure. These results underscore the profound impact of our work within this field of chemistry, reaching far beyond the confines of the laboratory. Furthermore, the synergy between our experimental research and computational calculations is pivotal for the strategic design of radical difunctionalization processes for highly strained molecules. This amalgamation of experimental and theoretical work not only advances our understanding of chemical transformations, but also offers valuable insights into the manipulation of high-energy substrates, paving the way for groundbreaking advancements in the realm of chemical synthesis.

METHODS

General Procedure for Diphosphination of Small Ring Molecules.

In an oven-dried round-bottom flask were placed phosphine oxide **1** (0.20 mmol, 1.0 equiv) and [Ir{dF(CF_3) ppy}$_2$(dtbbpy)]PF_6 (0.4 mg, 0.4 μmol, 0.20 mol %). DCE (1.5 mL), chlorophosphine **2** (0.20 mmol, 1.0 equiv) and Et_3N (28 μL, 0.20 mmol, 1.0 equiv) were added under nitrogen. After the resulting mixture was stirred at room temperature for 15 min, then 0 °C for 5 min, a substrate (0.20 mmol,

https://doi.org/10.1021/jacsau.4c00347
JACS Au 2024, 4, 3777−3787

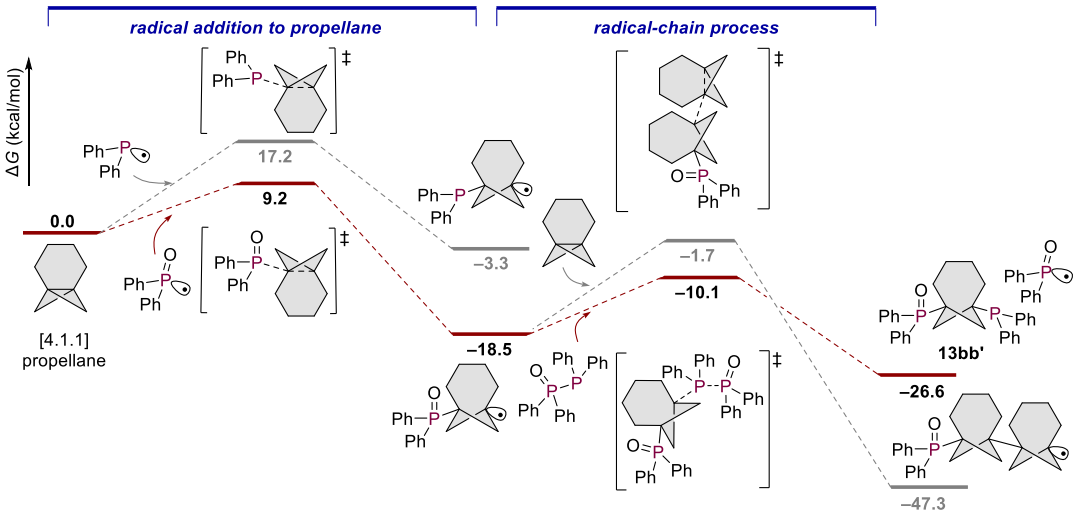

Figure 12. Plausible reaction mechanism based on DFT calculations for the 3CR with [4.1.1]propellane. The reaction diagrams were calculated at the UωB97X-D/Def2-SVP/SMD(DCM) level.

1.0 equiv) was added. The reaction mixture was stirred at 0 °C for 4 h under the irradiation of blue LED lights (PR160L-440 nm Kessil light ×2). The test tube was positioned between the two lamps, approximately 2 cm away from one of them. Sulfur (7.7 mg, 0.24 mmol, 1.2 equiv of S) was added into the reaction mixture, and the mixture was stirred for 1 h. After the solvent was evaporated to give the crude mixture, the crude product was purified by silica-gel column chromatography to afford the product.

■ ASSOCIATED CONTENT

Supporting Information

The Supporting Information is available free of charge at https://pubs.acs.org/doi/10.1021/jacsau.4c00347.

Additional experimental details, materials, and methods, including photographs of the experimental setup (PDF)

■ AUTHOR INFORMATION

Corresponding Author

Tsuyoshi Mita − *Institute for Chemical Reaction Design and Discovery (WPI-ICReDD), Hokkaido University, Sapporo, Hokkaido 001-0021, Japan; JST, ERATO Maeda Artificial Intelligence in Chemical Reaction Design and Discovery Project, Sapporo, Hokkaido 060-0810, Japan;* orcid.org/0000-0002-6655-3439; Email: tmita@icredd.hokudai.ac.jp

Authors

Chandu G. Krishnan − *Institute for Chemical Reaction Design and Discovery (WPI-ICReDD), Hokkaido University, Sapporo, Hokkaido 001-0021, Japan; JST, ERATO Maeda Artificial Intelligence in Chemical Reaction Design and Discovery Project, Sapporo, Hokkaido 060-0810, Japan;* orcid.org/0000-0002-1302-9975

Hideaki Takano − *Institute for Chemical Reaction Design and Discovery (WPI-ICReDD), Hokkaido University, Sapporo, Hokkaido 001-0021, Japan; JST, ERATO Maeda Artificial Intelligence in Chemical Reaction Design and Discovery Project, Sapporo, Hokkaido 060-0810, Japan;* orcid.org/0000-0003-0744-9292

Hitomi Katsuyama − *Institute for Chemical Reaction Design and Discovery (WPI-ICReDD), Hokkaido University, Sapporo, Hokkaido 001-0021, Japan; JST, ERATO Maeda Artificial Intelligence in Chemical Reaction Design and Discovery Project, Sapporo, Hokkaido 060-0810, Japan;* orcid.org/0000-0002-2753-0402

Wataru Kanna − *Department of Chemistry, Faculty of Science, Hokkaido University, Sapporo, Hokkaido 060-0810, Japan;* orcid.org/0000-0002-2931-6661

Hiroki Hayashi − *Institute for Chemical Reaction Design and Discovery (WPI-ICReDD), Hokkaido University, Sapporo, Hokkaido 001-0021, Japan; JST, ERATO Maeda Artificial Intelligence in Chemical Reaction Design and Discovery Project, Sapporo, Hokkaido 060-0810, Japan;* orcid.org/0000-0003-2081-6886

Complete contact information is available at: https://pubs.acs.org/10.1021/jacsau.4c00347

Author Contributions

The manuscript was written through contributions from all authors. All authors have given approval to the final version of the manuscript.

Notes

The authors declare no competing financial interest.

■ ACKNOWLEDGMENTS

Dr. Mingoo Jin and Kosuke Higashida are gratefully acknowledged for performing the X-ray crystallographic analyses. Miyu Harukawa, Makoto Tsurui, and Prof. Yasuchika Hasegawa of the Faculty of Engineering at Hokkaido University are greatly acknowledged for their contributions to preparing the Eu-based coordination polymer and conducting its crystallographic analysis. This work was financially supported by JST-ERATO (JPMJER1903), JSPS-WPI, and Grants-in-Aid for Scientific Research (B) (22H02069), Transformative Research Areas (A) (Digitalization-driven Transformative Organic Synthesis (Digi-TOS)) (22H05330), and Young Scientists (22K14673). T.M. thanks the Naito Foundation for financial support.

■ REFERENCES

(1) Hartwig, J. F. *Organotransition Metal Chemistry: From Bonding to Catalysis*; Univ Science Books, 2009.

(2) Orton, G. R. F.; Pilgrim, B. S.; Champness, N. R. The Chemistry of Phosphines in Constrained, Well-defined Microenvironments. *Chem. Soc. Rev.* **2021**, *50*, 4411−4431.
(3) Dierkes, P.; van Leeuwen, P. W. N. M. The Bite Angle Makes the Difference: A Practical Ligand Parameter for Diphosphine Ligands. *J. Chem. Soc., Dalton Trans.* **1999**, 1519−1530.
(4) van Leeuwen, P. W. N. M.; Kamer, P. C. J.; Reek, J. N. H.; Dierkes, P. Ligand Bite Angle Effects in Metal-Catalyzed C−C Bond Formation. *Chem. Rev.* **2000**, *100*, 2741−2770.
(5) Jia, G.; Puddephatt, R. J.; Scott, J. D.; Vittal, J. J. Organometallic Polymers with Gold(I) Centers Bridged by Diphosphines and Diacetylides. *Organometallics* **1993**, *12*, 3565−3574.
(6) Imhof, D.; Burckhardt, U.; Dahmen, K.-H.; Joho, F.; Nesper, R. Synthesis and Crystal Structure Determination of Bifunctional Phosphine-Linked Triplatinum Double-Cluster Complexes. *Inorg. Chem.* **1997**, *36*, 1813−1820.
(7) Van Calcar, P. M.; Olmstead, M. M.; Balch, A. L. Ligand Connected Metal Clusters. The Molecular Structures and Solid State Packing of $\{Ru_3(CO)_{11}\}_2$(bis(diphenylphosphino)ethane) and $\{Ru_3(CO)_{11}\}_2$(1,4-bis(diphenylphosphino)benzene). *Inorg. Chim. Acta* **1998**, *270*, 28−33.
(8) Li, D.; Feng, Q.; Feng, X.-L.; Cai, J.-W. A Photoluminescent Metallophane $[Cu_2(\mu\text{-dppb})_2(CH_3CN)_4](BF_4)_2$ with a Chair Conformation: Synthesis, Structural and Spectroscopic Studies. *Inorg. Chem. Commun.* **2003**, *6*, 361−364.
(9) Koshevoy, I. O.; Karttunen, A. J.; Tunik, S. P.; Haukka, M.; Selivanov, S. I.; Melnikov, A. S.; Serdobintsev, P. Y.; Khodorkovskiy, M. A.; Pakkanen, T. A. Supramolecular Luminescent Gold(I)−Copper(I) Complexes: Self-Assembly of the Au_xCu_y Clusters inside the $[Au_3(diphosphine)_3]^{3+}$ Triangles. *Inorg. Chem.* **2008**, *47*, 9478−9488.
(10) Koshevoy, I. O.; Karttunen, A. J.; Lin, Y.-C.; Lin, C.-C.; Chou, P.-T.; Tunik, S. P.; Haukka, M.; Pakkanen, T. A. Synthesis, Photophysical and Theoretical Studies of Luminescent Silver(I)−Copper(I) Alkynyl-Diphosphine Complexes. *Dalton Trans.* **2010**, *39*, 2395−2403.
(11) Rohacova, J.; Sekine, A.; Kawano, T.; Tamari, S.; Ishitani, O. Trinuclear and Tetranuclear Re(I) Rings Connected with Phenylene, Vinylene, and Ethynylene Chains: Synthesis, Photophysics, and Redox Properties. *Inorg. Chem.* **2015**, *54*, 8769−8777.
(12) Fernández-Moreira, V.; Cámara, J.; Smirnova, E. S.; Koshevoy, I. O.; Laguna, A.; Tunik, S. P.; Blanco, M. C.; Gimeno, M. C. Tuning the Energy Emission from Violet to Yellow with Bidentate Phosphine Gold(III) Complexes. *Organometallics* **2016**, *35*, 1141−1150.
(13) Tolman, C. A. Steric Effects of Phosphorus Ligands in Organometallic Chemistry and Homogeneous Catalysis. *Chem. Rev.* **1977**, *77*, 313−348.
(14) Bunten, K. A.; Chen, L.; Fernandez, A. L.; Poë, A. J. Cone Angles: Tolman's and Plato's. *Coord. Chem. Rev.* **2002**, *233*−*234*, 41−51.
(15) Bilbrey, J. A.; Kazez, A. H.; Locklin, J.; Allen, W. D. Exact Ligand Cone Angles. *J. Comput. Chem.* **2013**, *34*, 1189−1197.
(16) Casey, C. P.; Paulsen, E. L.; Beuttenmueller, E. W.; Proft, B. R.; Matter, B. A.; Powell, D. R. Electronically Dissymmetric DIPHOS Derivatives Give Higher n:i Regioselectivity in Rhodium-Catalyzed Hydroformylation Than Either of Their Symmetric Counterparts. *J. Am. Chem. Soc.* **1999**, *121*, 63−70.
(17) Carraz, C.-A.; Ditzel, E. J.; Orpen, A. G.; Ellis, D. D.; Pringle, P. G.; Sunley, G. J. Rhodium(I) Complexes of Unsymmetrical Diphosphines: Efficient and Stable Methanol Carbonylation Catalysts. *Chem. Commun.* **2000**, 1277−1278.
(18) Yue, W.-J.; Xiao, J.-Z.; Zhang, S.; Yin, L. Rapid Synthesis of Chiral 1,2-Bisphosphine Derivatives through Copper(I)-Catalyzed Asymmetric Conjugate Hydrophosphination. *Angew. Chem., Int. Ed.* **2020**, *59*, 7057−7062.
(19) RajanBabu, T. V.; Casalnuovo, A. L. Role of Electronic Asymmetry in the Design of New Ligands: The Asymmetric Hydrocyanation Reaction. *J. Am. Chem. Soc.* **1996**, *118*, 6325−6326.
(20) Nozaki, K. Unsymmetric Bidentate Ligands in Metal-Catalyzed Carbonylation of Alkenes. *Chem. Rec.* **2005**, *5*, 376−384.
(21) Thomas, A. A.; Speck, K.; Kevlishvili, I.; Lu, Z.; Liu, P.; Buchwald, S. L. Mechanistically Guided Design of Ligands That Significantly Improve the Efficiency of CuH-Catalyzed Hydroamination Reactions. *J. Am. Chem. Soc.* **2018**, *140*, 13976−13984.
(22) Wiberg, K. B. The Concept of Strain in Organic Chemistry. *Angew. Chem., Int. Ed.* **1986**, *25*, 312−322.
(23) Turkowska, J.; Durka, J.; Gryko, D. Strain Release − An Old Tool for New Transformations. *Chem. Commun.* **2020**, *56*, 5718−5734.
(24) Bellotti, P.; Glorius, F. Strain-Release Photocatalysis. *J. Am. Chem. Soc.* **2023**, *145*, 20716−20732.
(25) Blanchard, E. P., Jr.; Cairncross, A. Bicyclo[1.1.0]butane Chemistry. I. The Synthesis and Reactions of 3-Methylbicyclo[1.1.0]-butanecarbonitriles. *J. Am. Chem. Soc.* **1966**, *88*, 487−495.
(26) Cairncross, A.; Blanchard, E. P., Jr. Bicyclo[1.1.0]butane Chemistry. II. Cycloaddition Reactions of 3-Methylbicyclo[1.1.0]-butanecarbonitriles. The Formation of Bicyclo[2.1.1]hexanes. *J. Am. Chem. Soc.* **1966**, *88*, 496−504.
(27) Lampman, G. M.; Aumiller, J. C. Bicyclo[1.1.0]butane. *Org. Synth.* **1971**, *51*, 55.
(28) D'yachenko, A. I.; Abramova, N. M.; Zotova, S. V.; Nesmeyanova, O. A.; Bragin, O. V. New Synthesis of Bicyclo[1.1.0]-butane Hydrocarbons. *Russ. Chem. Bull.* **1985**, *34*, 1885−1889.
(29) Kelly, C. B.; Milligan, J. A.; Tilley, L. J.; Sodano, T. M. Bicyclobutanes: From Curiosities to Versatile Reagents and Covalent Warheads. *Chem. Sci.* **2022**, *13*, 11721−11737.
(30) Golfmann, M.; Walker, J. C. L. Bicyclobutanes as Unusual Building Blocks for Complexity Generation in Organic Synthesis. *Commun. Chem.* **2023**, *6*, 9.
(31) Tyler, J. L.; Aggarwal, V. K. Synthesis and Applications of Bicyclo[1.1.0]butyl and Azabicyclo[1.1.0]butyl Organometallics. *Chem.—Eur. J.* **2023**, *29*, No. e202300008.
(32) Kelly, C. B.; Colthart, A. M.; Constant, B. D.; Corning, S. R.; Dubois, L. N. E.; Genovese, J. T.; Radziewicz, J. L.; Sletten, E. M.; Whitaker, K. R.; Tilley, L. J. Enabling the Synthesis of Perfluoroalkyl Bicyclobutanes via 1,3 γ-Silyl Elimination. *Org. Lett.* **2011**, *13*, 1646−1649.
(33) Wiberg, K. B.; Taddell, S. T. Reactions of [1.1.1]Propellane. *J. Am. Chem. Soc.* **1990**, *112*, 2194−2216.
(34) Gianatassio, R.; Lopchuk, J. M.; Wang, J.; Pan, C.-M.; Malins, L. R.; Prieto, L.; Brandt, T. A.; Collins, M. R.; Gallego, G. M.; Sach, N. W.; Spangler, J. E.; Zhu, H.; Zhu, J.; Baran, P. S. Strain-release Amination. *Science* **2016**, *351*, 241−246.
(35) Shelp, R. A.; Walsh, P. J. Synthesis of BCP Benzylamines from 2-Azaallyl Anions and [1.1.1]Propellane. *Angew. Chem., Int. Ed.* **2018**, *57*, 15857−15861.
(36) Yu, S.; Noble, A.; Bedford, R. B.; Aggarwal, V. K. Methylenespiro[2.3]hexanes via Nickel-Catalyzed Cyclopropanations with [1.1.1]Propellane. *J. Am. Chem. Soc.* **2019**, *141*, 20325−20334.
(37) Lasányi, D.; Tolnai, G. L. Copper-Catalyzed Ring Opening of [1.1.1]Propellane with Alkynes: Synthesis of Exocyclic Allenic Cyclobutanes. *Org. Lett.* **2019**, *21*, 10057−10062.
(38) Kim, J. H.; Ruffoni, A.; Al-Faiyz, Y. S. S.; Sheikh, N. S.; Leonori, D. Divergent Strain-Release Amino-Functionalization of [1.1.1]-Propellane with Electrophilic Nitrogen-Radicals. *Angew. Chem., Int. Ed.* **2020**, *59*, 8225−8231.
(39) Zhang, X.; Smith, R. T.; Le, C.; McCarver, S. J.; Shireman, B. T.; Carruthers, N. I.; MacMillan, D. W. C. Copper-mediated Synthesis of Drug-like Bicyclopentanes. *Nature* **2020**, *580*, 220−226.
(40) Sterling, A. J.; Dürr, A. B.; Smith, R. C.; Anderson, E. A.; Duarte, F. Rationalizing the Diverse Reactivity of [1.1.1]Propellane through σ−π-Delocalization. *Chem. Sci.* **2020**, *11*, 4895−4903.
(41) Huang, W.; Keess, S.; Molander, G. A. Dicarbofunctionalization of [1.1.1]Propellane Enabled by Nickel/Photoredox Dual Catalysis: One-Step Multicomponent Strategy for the Synthesis of BCP-Aryl Derivatives. *J. Am. Chem. Soc.* **2022**, *144*, 12961−12969.

https://doi.org/10.1021/jacsau.4c00347
JACS Au 2024, 4, 3777−3787

(42) Kraemer, Y.; Ghiazza, C.; Ragan, A. N.; Ni, S.; Lutz, S.; Neumann, E. K.; Fettinger, J. C.; Nöthling, N.; Goddard, R.; Cornella, J.; Pitts, C. R. Strain-Release Pentafluorosulfanylation and Tetrafluoro(aryl)sulfanylation of [1.1.1]Propellane: Reactivity and Structural Insight. *Angew. Chem., Int. Ed.* **2022**, *61*, No. e202211892.
(43) Pickford, H. D.; Ripenko, V.; McNamee, R. E.; Holovchuk, S.; Thompson, A. L.; Smith, R. C.; Mykhailiuk, P. K.; Anderson, E. A. Rapid and Scalable Halosulfonylation of Strain-Release Reagents. *Angew. Chem., Int. Ed.* **2023**, *62*, No. e202213508.
(44) Nassir, M.; Ociepa, M.; Zhang, H.-J.; Grant, L. N.; Simmons, B. J.; Oderinde, M. S.; Kawamata, Y.; Cauley, A. N.; Schmidt, M. A.; Eastgate, M. D.; Baran, P. S. Stereocontrolled Radical Thiophosphorylation. *J. Am. Chem. Soc.* **2023**, *145*, 15088−15093.
(45) Frank, N.; Nugent, J.; Shire, B. R.; Pickford, H. D.; Rabe, P.; Sterling, A. J.; Zarganes-Tzitzikas, T.; Grimes, T.; Thompson, A. L.; Smith, R. C.; Schofield, C. J.; Brennan, P. E.; Duarte, F.; Anderson, E. A. Synthesis of *meta*-Substituted Arene Bioisosteres from [3.1.1]-Propellane. *Nature* **2022**, *611*, 721−726.
(46) Iida, T.; Kanazawa, J.; Matsunaga, T.; Miyamoto, K.; Hirano, K.; Uchiyama, M. Practical and Facile Access to Bicyclo[3.1.1]-heptanes: Potent Bioisosteres of *meta*-Substituted Benzenes. *J. Am. Chem. Soc.* **2022**, *144*, 21848−21852.
(47) Hamon, D. P. G.; Trenerry, V. C. Carbenoid Insertion Reactions: Formation of [4.1.1]Propellane. *J. Am. Chem. Soc.* **1981**, *103*, 4962−4965.
(48) Fuchs, J.; Szeimies, G. Synthese von [n.l.l]Propellanen (n = 2, 3, 4). *Chem. Ber.* **1992**, *125*, 2517−2522.
(49) Chen, M.; Cui, Y.; Chen, X.; Shang, R.; Zhang, X. C-F Bond Activation Enables Synthesis of Aryl Difluoromethyl Bicyclopentanes as Benzophenone-Type Bioisosteres. *Nat. Commun.* **2024**, *15*, 419.
(50) Locke, G. M.; Bernhard, S. S. R.; Senge, M. O. Nonconjugated Hydrocarbons as Rigid-Linear Motifs: Isosteres for Material Sciences and Bioorganic and Medicinal Chemistry. *Chem.—Eur. J.* **2019**, *25*, 4590−4647.
(51) Ma, X.; Pham, L. N. Selected Topics in the Syntheses of Bicyclo[1.1.1]Pentane (BCP) Analogues. *Asian J. Org. Chem.* **2020**, *9*, 8−22.
(52) Mykhailiuk, P. K. Saturated Bioisosteres of Benzene: Where to Go Next? *Org. Biomol. Chem.* **2019**, *17*, 2839−2849.
(53) Anderson, J. M.; Measom, N. D.; Murphy, J. A.; Poole, D. L. Bridge Functionalisation of Bicyclo[1.1.1]pentane Derivatives. *Angew. Chem., Int. Ed.* **2021**, *60*, 24754−24769.
(54) Shire, B. R.; Anderson, E. A. Conquering the Synthesis and Functionalization of Bicyclo[1.1.1]pentanes. *JACS Au* **2023**, *3*, 1539−1553.
(55) Takano, H.; Katsuyama, H.; Hayashi, H.; Kanna, W.; Harabuchi, Y.; Maeda, S.; Mita, T. A Theory-driven Synthesis of Symmetric and Unsymmetric 1,2-Bis(diphenylphosphino)ethane Analogues via Radical Difunctionalization of Ethylene. *Nat. Commun.* **2022**, *13*, 7034.
(56) Takano, H.; Katsuyama, H.; Hayashi, H.; Harukawa, M.; Tsurui, M.; Shoji, S.; Hasegawa, Y.; Maeda, S.; Mita, T. Synthesis of Bicyclo [1.1.1] pentane (BCP)-Based Straight-Shaped Diphosphine Ligands. *Angew. Chem., Int. Ed.* **2023**, *62*, No. e202303435.
(57) Maeda, S.; Ohno, K.; Morokuma, K. Systematic Exploration of the Mechanism of Chemical Reactions: The Global Reaction Route Mapping (GRRM) Strategy Using the ADDF and AFIR Methods. *Phys. Chem. Chem. Phys.* **2013**, *15*, 3683−3701.
(58) Maeda, S.; Taketsugu, T.; Morokuma, K. Exploring Transition State Structures for Intramolecular Pathways by the Artificial Force Induced Reaction Method. *J. Comput. Chem.* **2014**, *35*, 166−173.
(59) Maeda, S.; Harabuchi, Y.; Takagi, M.; Saita, K.; Suzuki, K.; Ichino, T.; Sumiya, Y.; Sugiyama, K.; Ono, Y. Implementation and Performance of the Artificial Force Induced Reaction Method in the GRRM17 Program. *J. Comput. Chem.* **2018**, *39*, 233−251.
(60) Maeda, S.; Harabuchi, Y. Exploring Paths of Chemical Transformations in Molecular and Periodic Systems: An Approach Utilizing Force. *WIREs Comput. Mol. Sci.* **2021**, *11*, No. e1538.
(61) Wiberg, K. B.; Walker, F. H.; Pratt, W. E.; Michl, J. [2.1.1]Propellane. Reaction of 1,4-Diiodobicyclo[2.1.1]hexane with *tert*-Butyllithium and with Potassium Atoms. *J. Am. Chem. Soc.* **1983**, *105*, 3638−3641.
(62) Eaton, P. E.; Temme, G. H. [2.2.2]Propellane System. *J. Am. Chem. Soc.* **1973**, *95*, 7508−7510.
(63) Wiberg, K. B.; Pratt, W. E.; Bailey, W. F. Reaction of 1,4-Diiodonorbornane, 1,4-Diiodobicyclo[2.2.2]octane, and 1,5-Diiodobicyclo[3.2.1]octane with Butyllithium. Convenient Preparative Routes to the [2.2.2]- and [3.2.1]Propellanes. *J. Am. Chem. Soc.* **1977**, *99*, 2297−2302.
(64) Weber, R. W.; Cook, J. M. General Method for the Synthesis of [n.3.3]Propellanes, $n \geq 3$. *Can. J. Chem.* **1978**, *56*, 189−192.
(65) Wender, P. A.; Dreyer, G. B. Synthetic Studies on Arene-Olefin Cycloadditions 4. Total Synthesis of (±)-Modhephene. *J. Am. Chem. Soc.* **1982**, *104*, 5805−5807.
(66) CCDC 2324260 (**6bb-*cis***), 2333566 (**$NiCl_2$(8bb-*cis*)**), and 2324261 (**12**) contain the supplementary crystallographic data for this paper. These data are provided free of charge by the Cambridge Crystallographic Data Centre; for details, see the Supporting Information (S34).
(67) Buonomo, J. A.; Eiden, C. G.; Aldrich, C. C. Scalable Synthesis of Hydrido-Disiloxanes from Silanes: A One-Pot Preparation of 1,3-Diphenyldisiloxane from Phenylsilane. *Synthesis* **2018**, *50*, 278−281.
(68) Buonomo, J. A.; Eiden, C. G.; Aldrich, C. C. Chemoselective Reduction of Phosphine Oxides by 1,3-Diphenyl-Disiloxane. *Chem.—Eur. J.* **2017**, *23*, 14434−14438.
(69) Bomfim, J. A. S.; de Souza, F. P.; Filgueiras, C. A. L.; de Sousa, A. G.; Gambardella, M. T. P. Diphosphine Complexes of Nickel: Analogies in Molecular Structures and Variety in Crystalline Arrangement. *Polyhedron* **2003**, *22*, 1567−1573.
(70) Strieth-Kalthoff, F.; James, M. J.; Teders, M.; Pitzer, L.; Glorius, F. Energy Transfer Catalysis Mediated by Visible Light: Principles, Applications, Directions. *Chem. Soc. Rev.* **2018**, *47*, 7190−7202.
(71) Wong, S. K.; Sytnyk, W.; Wan, J. K. S. The Flash Photolysis of Tetraphenyldiphosphine, Triphenylphosphine, and Diphenylphosphine in Alcohols. *Can. J. Chem.* **1971**, *49*, 994−1000.

https://doi.org/10.1021/jacsau.4c00347
JACS Au 2024, 4, 3777−3787